Magnetization studies in rare-earth orthochromites. VII. $LuCrO_3$†

R. M. Hornreich and S. Shtrikman
Department of Electronics, The Weizmann Institute of Science, Rehovot, Israel

B. M. Wanklyn
Clarendon Laboratory, Oxford, England

I. Yaeger*
Department of Electronics, The Weizmann Institute of Science, Rehovot, Israel
(Received 3 September 1975)

The magnetization and principal magnetic susceptibilities of $LuCrO_3$ are measured from ambient temperature down to 4.2°K. It is found that $LuCrO_3$ exhibits a weak ferromagnetic moment along the a crystallographic axis below $T_N = 111$°K. By applying a magnetic field along the antiferromagnetic c axis, the antiferromagnetic vector can be rotated smoothly in the a-c plane until it coincides with a at and above a critical field H_{cr}. This field increases with decreasing temperature, its value at $T = 4.2$°K being $H_{cr} = 3.6 \pm 0.4$ kOe. By comparing the temperature dependence of the spontaneous a-axis magnetization with that of the c-axis magnetization extrapolated to zero field, a quantitative separation between the Dzyaloshinsky-Moriya antisymmetric exchange (D) and single-ion anisotropy (A_{xz}) contributions to the canting is made. We find that $|A_{xz}/D| < 0.05$ for the case of $LuCrO_3$. As a consequence, a temperature-independent constant-canting-angle model is adopted. The temperature dependence of the reduced magnetization can then be analyzed using statistical-mechanical models developed for antiferromagnets. For $0.60 < T/T_N < 0.99$ the magnetization exhibits power-law behavior with $\beta \simeq 1/3$. For $T/T_N < 0.5$, its behavior is well described by spin-wave models. A comparison of the experimental results with theoretical curves calculated over the entire temperature range using molecular-field and several Green's-function models is also presented.

I. INTRODUCTION

The compound $LuCrO_3$, in conformity with other rare-earth orthochromites, crystallizes in an orthorhombically distorted perovskite structure (space group *Pbnm*) with four formula units per unit cell.[1] The exchange coupling between the Cr^{3+} nearest neighbors is predominantly antiferromagnetic and these ions order magnetically at a Néel temperature of $T_N = 111$ °K. Below this temperature $LuCrO_3$ exhibits a weak ferromagnetic moment.

From powder neutron-diffraction studies it has been reported[2] that the antiferromagnetic axis of the Cr^{3+} spins in $LuCrO_3$ at 4.2 and 80 °K lies in the a-c plane at an angle of 63° to the crystallographic a axis. The structure of the Cr^{3+} spins is thus, in the notation of Koehler *et al.*[3] and Bertaut,[4] primarily G_{xz} at these temperatures. This then implies that the weak ferromagnetic moment should have components along both the a and c axes and furthermore that the overall symmetry of the system is lowered from orthorhomic to monoclinc. In view of the directional behavior of the antiferromagnetic axis in other orthochromites[5] and in the isomorphic orthoferrites[6] (wherein the antiferromagnetic axis departs from a crystallographic direction only during a spin-reorientation process[7] which occurs over a limited temperature range) it is somewhat puzzling that in $LuCrO_3$ this axis should be fixed in a direction not prescribed by symmetry over a relatively wide temperature range. The clarification of this point was one of the objectives of our study.

Since the Lu^{3+} ions in $LuCrO_3$ are in a diamagnetic $^1S_0$ ground state, this compound's magnetic properties are dominated by the Cr spin system. Thus $LuCrO_3$ is a suitable material in which to study the behavior of the Cr spin system in the rare-earth orthochromites. Such a study is complicated in most of the orthochromites by the interactions between the Cr spin system and the paramagnetic rare-earth ions. The comparatively large contribution of the polarized rare-earth ions to the total magnetic moment and susceptibility, particularly at low temperatures, tends to dominate the relatively small Cr contributions.[5,8] In the case of $LuCrO_3$, however, the contributions of the diamagnetic Lu ions to the over-all magnetic properties will be negligible.

II. EXPERIMENTAL RESULTS

The magnetization and principal susceptibilities of flux-grown single crystals of $LuCrO_3$ (weighing a few tens of milligrams) were measured by means of motor-driven vibrating-sample magnetometers.[9] The measurements were carried out in the 4.2–300 °K temperature range. The sample was cooled by a stream of helium gas inside a double-walled glass cryostat. Constant temperatures were maintained by means of a temperature controller operated by a magnetic valve. In addition, measurements

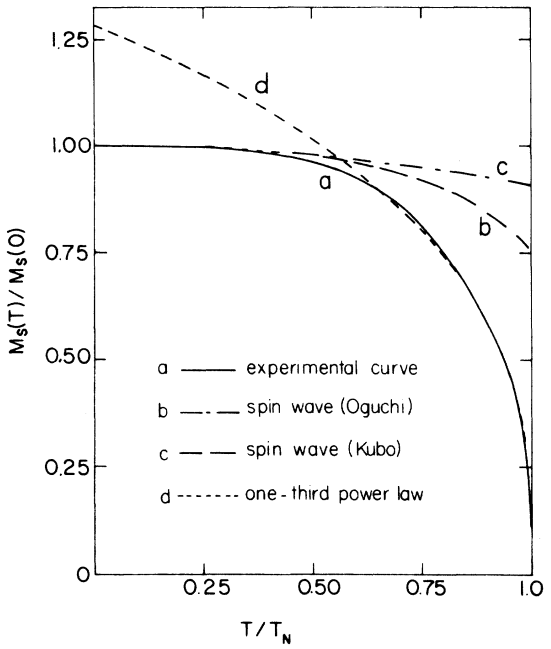

FIG. 1. Reduced spontaneous magnetization $M_s(T)/M_s(0)$ of $LuCrO_3$ in the G_zF_x phase (which is equal within the experimental error to the zero-field-extrapolated magnetization in the induced G_xF_z phase) as a function of the reduced temperature T/T_N. (a) Experimental results; (b) spin-wave theory at low temperature (Oguchi); (c) spin-wave theory at low temperature (Kubo); (d) one-third-power law near T_N.

at 4.2 °K were taken with the sample immersed in liquid helium. The reported results were compiled from (i) magnetization measurements versus temperature recorded at various fixed magnetic fields while heating or cooling the sample and (ii) curves of magnetization versus applied field recorded at fixed temperatures.

The spontaneous magnetization of $LuCrO_3$ is shown in Fig. 1. Below its ordering temperature, $T_N = 111 \pm 1$ °K, and down to 4.2 °K the magnetization, to within an experimental error of ± 3°, was found to lie in the crystallographic a direction. (The crystallographic a axis was determined from a knowledge of the symmetry and morphological features of the crystals.[1,10]) Thus our results differ from those reported from powder neutron-diffraction studies.[2] The spontaneous magnetization extrapolated to 0 °K was 360 ± 20 emu/mole. By applying a relatively small external magnetic field parallel to the c axis the spontaneous magnetization could be aligned along c. An example of this field-induced phase transition is shown in Fig. 2. The magnitude of the critical field H_{cr} required to induce the phase transition was found to decrease monotonically as the temperature was increased. At 4.2 ° K H_{cr} was approximately 4 kOe. At temperatures above 40 °K it was difficult to trace the spin-reorientation process, as it was obscured to a large extent by the usual low-field demagnetizing effects. It was found that the ferromagnetic moment extrapolated to zero field in the field-induced G_xF_z phase coincided, to within the experimental error of ± 5%, with the G_zF_x-phase spontaneous magnetization.

The magnetic susceptibility measured along each of the principal crystallographic directions of $LuCrO_3$ is shown in Fig. 3. Note that the high-field c-axis susceptibility was measured in the field-induced G_xF_z phase. The field-induced spin-reorientation process is reflected in the low-field c-axis susceptibility data. The slight rise found in the a-axis susceptibility at low temperatures is probably due to isolated paramagnetic impurities.

III. ANALYSIS

The relatively simple spin structure of the ordered Cr moments in $LuCrO_3$ makes it possible to compare the experimental results with those obtained from different statistical-mechanical models and thus to obtain some indication of their applicability to the rare-earth orthochromites in general. We shall therefore analyze the experimental data presented in Sec. II using molecular-field, spin-wave, and Green's-function models, and a power-law critical behavior for the sublattice magnetization. The calculations will be based on a single-ion, two-sublattice description for the Cr

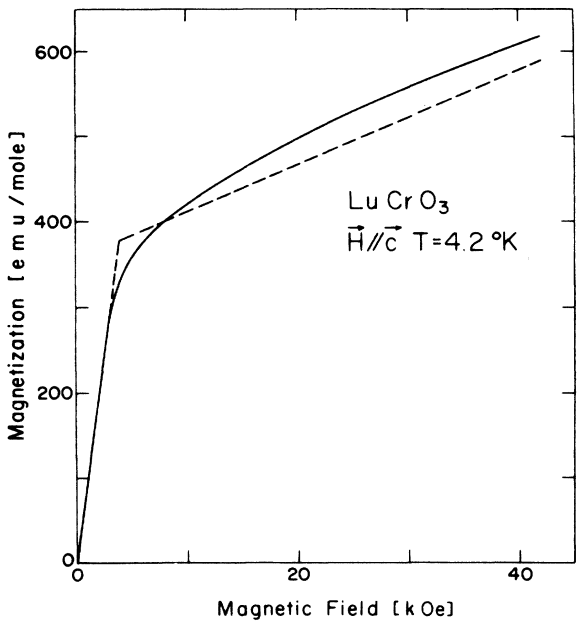

FIG. 2. Magnetization of $LuCrO_3$ as a function of an applied magnetic field along the orthorhombic c direction at $T = 4.2$ °K.

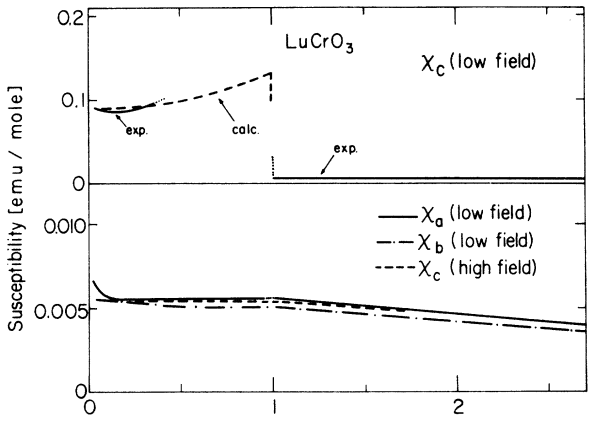

FIG. 3. Principal magnetic susceptibilities of $LuCrO_3$ as a function of the reduced temperature T/T_N. The subscripts a, b, and c refer to the orthorhombic crystallographic axes. All of the curves in the lower part of the figure are experimental. The dotted regions in the χ_a(low field) and χ_c(low field) curves indicate interpolations and extrapolations.

moments. In this approximation the Hamiltonian of the Cr spins can be written in the form[11]

$$\mathcal{H} = 2J\sum_{(ij)} \vec{S}_i \cdot \vec{S}_j - \vec{D} \cdot \sum_{(ij)} \vec{S}_i \times \vec{S}_j - A_{xz}\Big(\sum_i S_{ix} S_{iz} - \sum_j S_{jx} S_{jz}\Big) - K_2 \sum_l S_{lz}^2 - g\mu_B \vec{H} \cdot \sum_l \vec{S}_l, \qquad (1)$$

where S_i is a spin in one sublattice, S_j belongs to the other sublattice, S_l belongs to either of the sublattices, the l summation extends over all spins, and the (ij) summation extends over pairs of nearest-neighbor spins. The first and second terms are isotropic nearest-neighbor and Dzyaloshinsky-Moriya exchange interactions, respectively. The third and fourth terms are due to quadratic anisotropy. As a result of the third term, the two sublattices will have different easy directions in the a-c plane. The fourth fixes c as the antiferromagnetic axis of the system. The final term is the direct interaction of the spins with the external magnetic field. The Dzyaloshinsky vector $\vec{D}$ is in the $-b$ direction[12] and in the absence of an external magnetic field the spins of both sublattices are confined to lie in the a-c plane. The subscripts x, y, and z refer to the orthorhombic a, b, and c axes, respectively. The four constants in the Hamiltonian, J, D, A_{xz}, and K_2, will be regarded as adjustable parameters, to be determined by fitting the model calculations to the experimental data.

A. Molecular-field model

In the molecular-field approximation the weak moment M_{sa} of $LuCrO_3$ in the $G_z F_x$ phase and the zero-field extrapolated moment M_{sc} in the field-induced $G_x F_z$ phase are given by

$$M_{si}(T) = Ng\mu_B S(\langle S_\zeta\rangle/S)\sin\alpha_i \quad i=a,c, \qquad (2)$$

where N is Avogadro's number, $g=2$ is the gyromagnetic factor of the Cr moments, μ_B is the Bohr magneton, and $\langle S_\zeta\rangle/S$ is the reduced spontaneous magnetization per $S=\frac{3}{2}$ spin as a function of the absolute temperature T. (ζ is the direction of the local effective field on the given spin.) The angle α_i is the canting angle of the Cr sublattice moments away from the antiferromagnetic axis. For small canting angles the magnitude of α_i is given by[11]

$$2\alpha_i = \frac{D}{2J} \pm \frac{A_{xz}}{2J}\,\frac{3S}{2S-1}\,\frac{\langle S_\zeta^2\rangle - \frac{1}{3}S(S+1)}{\langle S_\zeta\rangle^2}, \qquad (3)$$

where $\langle\ \rangle$ denotes a statistical average over the $2S+1$ spin states and the upper and lower algebraic signs apply to the $G_x F_z$ and the $G_z F_x$ phases, respectively.

Experimentally, we find that M_{sa} and M_{sc} are equal to within an estimated maximum experimental error of 5% between 4.2 and $T_N = 111\,^\circ$K. This implies that $|A_{xz}/D| < 0.05$, i.e., that the anisotropy contribution to the Cr canting is negligible compared with that owing to antisymmetric exchange. It follows that the canting angle is temperature independent for all $T < T_N$ and that the temperature dependence of the spontaneous moment is identical to that of the sublattice magnetization. We can therefore compare the temperature dependence of the reduced sublattice magnetization, as obtained from the $S=\frac{3}{2}$ Brillouin function, with that of the measured weak ferromagnetic moment of $LuCrO_3$. The results are shown in Fig. 4. The canting angle α, as determined by fitting Eq. (2) to the measured moment of $LuCrO_3$ at 4.2 °K, is $\alpha = 21.3 \pm 1.0$ mrad for both phases. The value of J, as obtained from the molecular-field expression

$$T_N = 2JzS(S+1)/3k, \qquad (4a)$$

is $J/k = 7.4\,^\circ$K. This is the value used for the molecular-field calculation shown in Fig. 4. Here $z=6$ is the number of nearest Cr^{3+} neighbors and k is Boltzmann's constant. Alternately, J may be found from the perpendicular susceptibility

$$\chi_\perp = Ng^2\mu_B^2/4Jz. \qquad (4b)$$

Taking the experimental value, $\chi_\perp = (5.5 \pm 0.5)\times 10^{-3}$ emu/mole Oe (see Fig. 3); Eq. (4b) yields $J/k = 11.4 \pm 1.0\,^\circ$K. This value of J will be used for the remainder of our molecular-field analysis. The reasons for this choice will be discussed in Sec. IV. The value of D can now be determined from the canting angle α, using Eq. (3). The result is $D/k = 0.96 \pm 0.10\,^\circ$K.

We shall now use those parameter values to analyze the field-induced $G_z F_x - G_x F_z$ phase transition. We restrict our analysis to temperatures $T \ll T_N$.

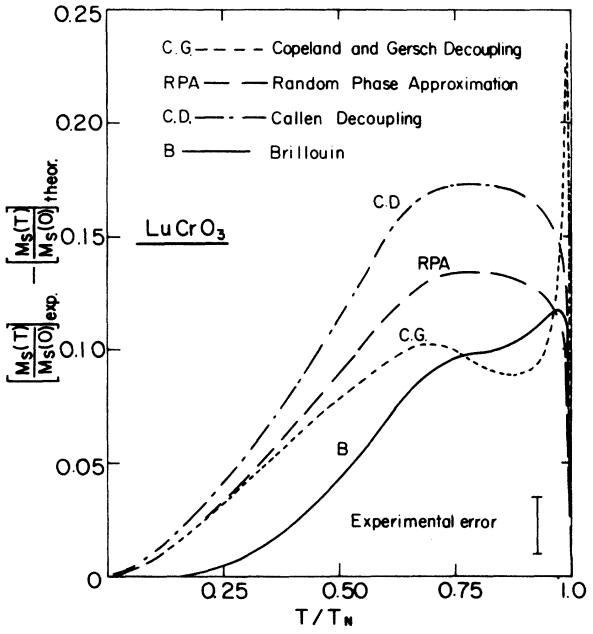

FIG. 4. Difference between the experimental and various theoretical values of the reduced spontaneous magnetization of $LuCrO_3$ as a function of the reduced temperature T/T_N.

In this region the sublattice magnetization vectors are essentially saturated and the free energy F can be taken as

$$F = U, \tag{5}$$

where U is the Hamiltonian of Eq. (1) with the spins regarded as classical vectors. We set $A_{xz} = 0$ in accordance with our previous results and define

$$H_E = 2JzS/g\mu_B, \quad H_D = DzS/g\mu_B, \quad H_K = 2K_2S/g\mu_B. \tag{6}$$

Using Eq. (6) and the J and D values found previously, we obtain $H_E = 990 \pm 100$ kOe and $H_D = 42 \pm 4$ kOe. We now minimize F with respect to the canting angle α and the angle θ between the antiferromagnetic axis and c for the case of a field H_z applied parallel to c. Assuming $H_K \ll H_D \ll H_E$, we obtain

$$\alpha = (H_D + H_z \sin\theta)/(2H_E), \tag{7}$$

where

$$\sin\theta \begin{cases} = H_z H_D/(2H_K H_E - H_z^2), & \text{for } H_z \le H_{cr}, \\ = 1, & \text{for } H_z \ge H_{cr}. \end{cases} \tag{8}$$

Here H_{cr} is the critical field above which only the G_xF_z phase is present. This field is given by

$$H_{cr} = \tfrac{1}{2}[-H_D + (H_D^2 + 8H_K H_E)^{1/2}]. \tag{9}$$

The component of the magnetization in the c direction is given by

$$M_c(H_z) = Ng\mu_B S\alpha \sin\theta, \tag{10}$$

where α and θ are given by Eqs. (7) and (8), respectively. From a best least-squares fit of Eq. (10) to the experimental data at 4.2 °K (see Fig. 2) the value of the remaining parameter H_K was found to be $H_K = 84 \pm 10$ Oe. This is equivalent to $K_2/k = (3.8 \pm 0.4) \times 10^{-3}$ °K. Using these values for H_E, H_D, and H_K, Eq. (9) yields $H_{cr} = 3.6 \pm 0.4$ kOe, in good agreement with the experimental data. Here and henceforth all quoted errors are statistical and correspond to two standard deviations.

The spin-reorientation process also contributes to the low-field magnetic susceptibility parallel to the antiferromagnetic axis. At temperatures $T/T_N \ll 1$ this susceptibility will be due entirely to the rotation of the antiferromagnetic axis. It is then given by[13]

$$\chi_c(\text{low field}, T = 0\ ^\circ\text{K}) = Ng^2\mu_B^2 D^2/32J^2K_2 = 0.09 \text{ emu/mole Oe}. \tag{11}$$

It follows from Eq. (11) that demagnetizing corrections are negligible.

The temperature dependence of the low-field parallel susceptibility can be found using the equations derived for the case of $YFeO_3$.[13] In adopting these equations to $LuCrO_3$ the roles of the a and c axes were interchanged (in $YFeO_3$ the spin reorientation is from a to c when a magnetic field is applied along a). The resulting calculated temperature dependence of χ_c(low field) is shown in Fig. 3.

B. Spin-wave models

When the canting angle is temperature independent, the temperature dependence of the sublattice magnetization is identical to that of the spontaneous magnetization for all $T < T_N$. We can therefore compare the results of spin-wave models of antiferromagnetic behavoir with the measured spontaneous magnetization of $LuCrO_3$ at low temperatures.

Using a spin-wave treatment, the low-temperature reduced sublattice magnetization of a simple-cubic antiferromagnet with negligible anisotropy has been found by Kubo[14] to be

$$\langle S_z\rangle/S = 1 - (S - 0.078)^{-1}\tfrac{1}{2}\sqrt{3}(kT/2zJS)^2. \tag{12}$$

For the case of $LuCrO_3$, this reduces to

$$\langle S_z\rangle/S = 1 - 1.880 \times 10^{-3}(kT/J)^2. \tag{13}$$

A best least-squares fit of Eq. (13) to the experimetal data for $T/T_N \le 0.5$ was obtained with $J = 15.8 \pm 2.4$ °K. This value is in poor agreement with

that derived from the perpendicular susceptibility $\chi_\perp$ in the molecular-field approximation (the same expression for $\chi_\perp$ is obtained by Kubo[14]). However, as shown in Fig. 1 the calculated curve agrees quite well with the experimental results for $T/T_N \leq 0.5$.

The behavior of the antiferromagnetic sublattice magnetization has also been studied by Oguchi[15] using spin-wave theory. In his approach, the reduced sublattice magnetization is calculated as a series expansion in powers of $(kT/J)^2$. For the case of $LuCrO_3$ his results can be expressed

$$\langle S_\xi\rangle/S = 1 - 1.758\times10^{-3}(kT/J)^2 - 1.994\times10^{-5}(kT/J)^4 - 1.126\times10^{-6}(kT/J)^6, \quad (14)$$

keeping terms up to sixth order in kT/J. The best-fit value of J obtained using Eq. (14) in the range $T/T_N \leq 0.5$ was 16.3 ± 1.8 °K. This result is in agreement with that obtained from Kubo's expression for $\langle S_\xi\rangle/S$ but again differs from that found from the molecular-field expression for $\chi_\perp$. The calculated curve obtained using Eq. (14) is in good agreement with the experimental data for $T/T \leq 0.5$ (see Fig. 1).

We have also evaluated J using Obuchi's expression for $\chi_\perp$.[15] This calculation gives $J/k = 10.4 \pm 1.0$ °K. As might be expected, this is essentially the same as the result found using Eq. (4b).

C. Green's-function models

We have also calculated $\langle S_\xi\rangle/S$ as a function of temperature using the method of Green's functions. Results were obtained using three different decoupling schemes. We use the notation of Copeland and Gersch.[16] They have shown that the reduced sublattice magnetization of a Heisenberg antiferromagnet [i.e., taking into consideration only the first term in the Hamiltonian of Eq. (1)] is given by

$$\frac{\langle S_\xi\rangle}{S} = \frac{1}{S}\,\frac{(S-\phi_0)(1+\phi_0)^{2S+1} + (S+1+\phi_0)\phi_0^{2S+1}}{(1+\phi_0)^{2S+1} - \phi_0^{2S+1}}, \quad (15)$$

where

$$\phi_\delta = \frac{1}{N}\sum_{\vec{k}} \frac{e^{i\vec{k}\cdot\vec{\delta}}}{\exp[(\gamma_0-\gamma_k)/R]-1}, \quad (16)$$

$$\gamma_k = \sum_{\vec{\delta}} e^{i\vec{k}\cdot\vec{\delta}}. \quad (17)$$

The sums on $\vec{k}$ and $\vec{\delta}$ in Eqs. (16) and (17) are over the first Brillouin zone and the vectors joining a magnetic lattice site to its nearest neighbors, respectively.

The relation between $\langle S_\xi\rangle$ and the reduced temperature T/T_N is

$$T/T_N = 2(R/zX)\langle S_\xi\rangle(1+2\psi\phi_\delta), \quad (18)$$

with

$$X = kT_N/zJ. \quad (19)$$

Here R is an auxiliary computational parameter. The values of X and the termination fuction ψ depend upon the particular decoupling scheme used. For a simple-cubic antiferromagnet, $X = 1.648$ and $\psi = 0$ in the random-phase approximation[17] (RPA), $X = 1.9565$, $\psi = \langle S_\xi\rangle/2S^2$ using Callen (CD) decoupling[17], and $X = 1.667$, $\psi = \langle S_\xi\rangle^3/2S^4$ using Copeland-Gersch (CG) decoupling.[16] For each decoupling scheme, the exchange integral J was chosen to make the calculated value of T_N equal to the experimental value.

In the rare-earth orthochromites, the Cr ions form a simple-cubic lattice. Replacing the sum of $\vec{k}$ in Eq. (16) by an integral gives

$$\phi_\delta = \left(\frac{a}{\pi}\right)^3 \int_0^{\pi/a}\int_0^{\pi/a}\int_0^{\pi/a} \frac{\cos(\vec{k}\cdot\vec{\delta})\,dk_x\,dk_y\,dk_z}{\exp[(\gamma_0-\gamma_k)/R]-1}. \quad (20)$$

For a simple-cubic lattice of side a,

$$\gamma_k = 2[\cos(k_x a)+\cos(k_y a)+\cos(k_z a)], \quad (21)$$

and, obviously, $\gamma_0 = 6$. For the case of $LuCrO_3$, $a = 3.7375$ Å.

The procedure used to calculate $\langle S_\xi\rangle/S$ as a function of T/T_N was to choose a value for the parameter R and then to evaluate ϕ_0 and ϕ_δ numerically. Following this, $\langle S_\xi\rangle/S$, ψ, and T/T_N were calculated. This process was then repeated for different values of R and for each of the three decoupling schemes. The results are shown in Fig. 4 and the values of J are listed in Table I. Clearly the CG decoupling scheme yields the best fit to the experimental data. Note that the over-all difference between theory and experiment in Fig. 4 is not significantly different for Green's-function and molecular-field models. However, the description of the

TABLE I. Values of the exchange integral J/k in $LuCrO_3$.

Method of Evaluation	J/k (°K)
Molecular field (T_N)	7.4
High-temperature series expansion (T_N)	10.3
Green's functions (RPA) (T_N)	11.2
Green's functions (CD) (T_N)	9.4
Green's functions (CG) (T_N)	11.1
Kubo's spin waves and molecular field ($\chi_\perp$)	11.4 ± 1.0
Oguchi's spin waves ($\chi_\perp$)	10.4 ± 1.0
Kubo's spin waves ($\langle S_\xi\rangle/S$)	15.8 ± 2.5
Oguchi's spin waves ($\langle S_\xi\rangle/S$)	16.3 ± 1.8

temperature dependence of the spontaneous moment by the Brillouin function was obtained, as noted earlier, by choosing $J/k = 7.4\,^{\circ}\mathrm{K}$. If a more realistic value of J had been chosen, the disagreement between the molecular-field calculation and experiment would have been considerably greater than that found for any of the Green's-function theories.

D. Power-law behavior

The reduced sublattice magnetization as a function of temperature T near the Néel point has been found, both theoretically[18–21] and experimentally,[22–28] to behave as

$$\langle S_z \rangle / S = d(1 - T/T_N)^{\beta}, \tag{22}$$

where d and β are constants. A least-squares fit of Eq. (22) to the experimental spontaneous magnetization of $LuCrO_3$ in the temperature range $0.60 < T/T_N < 0.99$ yielded $d = 1.28 \pm 0.01$ and $\beta = 0.337 \pm 0.003$. The magnetization calculated using these values and Eq. (22) is shown in Fig. 1. We see that the magnetization of $LuCrO_3$ follows Eq. (22) over a wide temperature range near T_N with a value of β close to $\frac{1}{3}$. This is in agreement with the Green's-function theories in the RPA and CD decoupling approximations. (See, for example, Table III of Ref. 28.) Similar results have been reported for the temperature dependence of the reduced hyperfine field in the isomorphous rare-earth orthoferrites $RFeO_3$.[26,28] A β value close to $\frac{1}{2}$ has been reported from magnetization and susceptibility studies on $YFeO_3$ in the range $0.996 < T/T_N < 1.003$.[27] However, it was found that $\beta \simeq \frac{1}{3}$ in a temperature range further away from T_N.[27]

IV. DISCUSSION

Since the spontaneous ferromagnetic moment of $LuCrO_3$ lies along the crystallographic a axis, it follows that this compound's spin structure is $G_z F_x$. This conclusion thus differs from that reported from neutron-diffraction studies on $LuCrO_3$ power.[2] Similar differences have been reported for $TmFeO_3$,[29,30] $NdCrO_3$,[31] $YbCrO_3$,[32] and $TmCrO_3$.[8] Since the directions of the spontaneous magnetization and antiferromagnetic axis determined by single-crystal magnetization measurements are unambiguous, it is clear that the results of neutron-diffraction studies on powder samples may be consistent with more than one spin structure. This is particularly true when the details of the spin-distribution function are not known.[33]

In Sec. III, the $LuCrO_3$ data have been compared with the predictions of several statistical-mechanical models of antiferromagnetism. We have seen that a relatively simple molecular-field model gives a good description of the main features of the temperature and field dependence of the spontaneous magnetization and magnetic susceptibility of $LuCrO_3$. However, this result is somewhat misleading, as it was based upon determining the exchange constant J from the Néel point. In fact, this yields a very poor value for J (see Table I). For this reason, the remainder of the molecular-field analysis was based upon the value of J obtained from the experimental perpendicular-susceptibility data. This latter value is in good agreement with values derived from the other models considered by us and also with that found using the results of high-temperature series expansions[34] (see Table I). With this additional consideration, we conclude that the Green's-function models give the best overall description of the temperature dependence of the spontaneous magnetization.

TABLE II. Comparison of $LuCrO_3$ with $YCrO_3$ and $YFeO_3$ (α—canting angle; H_E, H_D, H_K, and $H'_K - 0\,^{\circ}\mathrm{K}$ Heisenberg exchange, Dzyaloshinsky-Moriya antisymmetric exchange, quadratic anisotropy, and quartic anisotropy fields, respectively; H_{cr}—critical field).

	$LuCrO_3$ (This work)	$YCrO_3$ (Ref. 34[a])	$YFeO_3$ (Ref. 34[a])	$YFeO_3$ (Ref. 13)
H_E (kOe)	990 ± 100	2300	6400	5200[a]
H_D (kOe)	42 ± 4	61	140	125[a]
H_K (kOe)	0.084 ± 0.010	0.88	1.2	1.1[a] 2.08[b] 0.086[a]
H'_K (kOe)	0	0	0.26	0.36[b]
α (mrad)	21.3 ± 1.0	13.2	10.9	12
H_{cr} (kOe)	3.55 ± 0.40	40	74	

[a]From the field dependence of the magnetization at 4.2°K.

[b]From the temperature dependence of the spontaneous magnetization and/or magnetic susceptibility.

In our analysis we did not include a quartic anisotropy term of the form $-K_4 \sum_i S_{iz}^4$ in Eq. (1) though such a term was necessary for the case of $YFeO_3$.[13,35] (The quartic anisotropy field at 0 °K in $YFeO_3$, $H'_K = 2K_4 S^3/g\mu_B$, is given in Table II.) Our results thus indicate that a quadratic anisotropy model is adequate to describe the magnetic behavior of $LuCrO_3$. This was also found to be true for the case of $YCrO_3$.[35] Note that this does not imply that the quadratic anisotropy energy is entirely magnetocrystalline in origin. In fact, a direct calculation yields a dipolar contribution to K_2/k of $-58 \times 10^{-3}\,^{\circ}\mathrm{K}$, indicating that the effective K_2 appearing in Eq. (1) has both dipolar and magnetocrystalline components that are nearly equal in magnitude and opposite in sign. A comparison of our results with those reported for $YCrO_3$ and $YFeO_3$ is given in Table II.

Finally, $LuCrO_3$ is the only known compound among the orthochromites and orthoferrites con-

taining diamagnetic rare-earth ions that spontaneously orders with its antiferromagnetic axis along c.[12,13,35-37] When a magnetic field is applied along c the system appears to undergo two second-order phase transitions, from $G_z F_x$ to a mixed phase to $G_x F_z$. The second-order nature of the latter transition is in accord with the predictions of molecular-field studies.[38,39] To illustrate this let us consider the phase transition shown in Fig. 2. The field-induced phase transition at 0 °K is expected to be of first or second order according to whether H_D is less or greater than H_D^{crit}, where $H_D^{crit} = 4.5\sqrt{2}\,(H_K/H_E)^{3/2} H_E$. We find $H_D^{crit} = 5$ Oe and $H_D = 42$ kOe, in agreement with the observed second-order character of the phase transition.

ACKNOWLEDGMENT

We are grateful to D. Gordon for several helpful discussions and suggestions during the course of this work.

*Work supported in part by the Commisison for Basic Research of the Israel Academy of Sciences and Humanities.

†Present address: Dept. of Physics, The University of Manitoba, Winnipeg, Canada.

[1]S. Geller and E. A. Wood, Acta Crystallogr. 9, 563 (1956); S. Geller, J. Chem. Phys. 24, 1236 (1956); E. F. Bertaut and F. Forrat, J. Phys. Rad. 17, 129 (1956).

[2]E. F. Bertaut, J. Mareschal, G. de Vries, R. Aleonard, R. Pauthenet, J. P. Rebouillat, and V. Zarubicka, IEEE Trans. Magn. 2, 453 (1966).

[3]W. C. Koehler, E. O. Wollan, and M. K. Wilkinson, Phys. Rev. 118, 58 (1960).

[4]E. F. Bertaut, in *Magnetism*, edited by G. T. Rado and H. Suhl (Academic, New York, 1963), Vol. III, p. 149.

[5]G. Gorodetsky, L. M. Levinson, S. Shtrikman, and B. Wanklyn, Phys. Rev. 187, 637 (1969).

[6]R. M. Hornreich, B. Wanklyn, and I. Yaeger, Int. J. Magn. 2, 77 (1972); K. Tsushima, K. Aoyagi, and S. Sugano, J. Appl. Phys. 41, 1238 (1970).

[7]L. M. Levinson, M. Luban, and S. Shtrikman, Phys. Rev. 187, 715 (1969).

[8]R. M. Hornreich, B. M. Wanklyn, and I. Yaeger, Int. J. Magn. 4, 313 (1973).

[9]P. J. Flanders and W. D. Doyle, Rev. Sci. Instrum. 33, 691 (1962).

[10]M. Eibschütz, Acta Crystallogr. 19, 337 (1965); P. Coppens and M. Eibschütz, *ibid.* 19, 524 (1965).

[11]G. F. Herrmann, Phys. Rev. 133, A1334 (1964).

[12]D. Treves, J. Appl. Phys. 36, 1033 (1965); Phys. Rev. 125, 1843 (1962).

[13]G. Gorodetsky, S. Shtrikman, Y. Tenenbaum, and D. Treves, Phys. Rev. 181, 823 (1969).

[14]R. Kubo, Phys. Rev. 87, 568 (1952).

[15]T. Oguchi, Phys. Rev. 117, 117 (1960).

[16]J. A. Copeland and H. A. Gersch, Phys. Rev. 143, 236 (1966).

[17]F. B. Anderson and H. B. Callen, Phys. Rev. 136, A1068 (1964).

[18]C. N. Yang, Phys. Rev. 85, 808 (1952).

[19]G. A. Baker, Jr., Phys. Rev. 124, 768 (1961).

[20]J. W. Essam and M. E. Fisher, J. Chem. Phys. 38, 802 (1963).

[21]E. Callen and H. B. Callen, J. Appl. Phys. 36, 1140 (1965).

[22]P. Heller and G. Benedek, Phys. Rev. Lett. 8, 428 (1962).

[23]P. Heller and G. Benedek, Phys. Rev. Lett. 14, 71 (1965).

[24]D. G. Howard, B. D. Dunlap, and J. G. Dash, Phys. Rev. Lett. 15, 628 (1965).

[25]R. S. Preston, S. S. Hanna, and J. Heberle, Phys. Rev. 128, 2207 (1962).

[26]M. Eibschütz, S. Shtrikman, and D. Treves, Solid State Commun. 4, 141 (1966).

[27]G. Gorodetsky, S. Shtrikman, and D. Treves, Solid State Commun. 4, 147 (1966).

[28]M. Eibschütz, S. Shtrikman, and D. Treves, Phys. Rev. 156, 562 (1967).

[29]J. A. Leake, G. Shirane, and J. P. Remeika, Solid State Commun. 6, 15 (1968).

[30]R. C. LeCraw, R. Wolfe, E. M. Gyorgy, E. B. Hagedorn, J. C. Hensel, and J. P. Remieka, J. Appl. Phys. 39, 1019 (1968).

[31]R. M. Hornreich, Y. Komet, R. Nolan, B. M. Wanklyn, and I. Yaeger, Phys. Rev. B 12, 5094 (1975).

[32]S. Shtrikman, B. M. Wanklyn, and I. Yaeger, Int. J. Magn. 1, 327 (1971).

[33]Z. Friedman, H. Pinto, H. Shaked, G. Gorodetsky, and S. Shtrikman, Int. J. Magn. 2, 409 (1971).

[34]G. S. Rushbrooke and P. J. Wood, Mol. Phys. 6, 409 (1963).

[35]I. S. Jacobs, H. F. Burne, and L. M. Levinson, J. Appl. Phys. 42, 1631 (1971).

[36]K. Tsushima, I. Takemura, and S. Osaka, Solid State Commun. 7, 71 (1969).

[37]V. M. Judin and A. B. Sherman, Solid State Commun. 4, 661 (1966).

[38]R. M. Hornreich, K. A. Penson, and S. Shtrikman, J. Phys. Chem. Solids 33, 433 (1972).

[39]J. Berger and R. M. Hornreich, J. Phys. Chem. Solids, 34, 2011 (1973).